

Tube Integrability in a Time-Dependent Nonlinear Oscillator

Johannes Hagel

Alexander-von-Humboldt-Gymnasium Neuss
Bergheimer Straße 233, 41464 Neuss, Germany
johannes.hagel@gmail.com

1 November 2025

Abstract

We study the nonlinear oscillator $z'' + \omega^2 z + g(t)z^2 = 0$ with a time-dependent coefficient $g(t)$. We show that this equation admits an exact quadratic invariant $I(z, p, t)$ provided that $g(t) = \alpha_2(t)^{-5/2}$ and $\alpha_2(t)$ satisfies a nonlinear third-order differential equation. The resulting invariant constrains the dynamics to a smooth two-dimensional surface in the extended phase space (z, p, t) . If $\alpha_2(t)$ is periodic, this surface forms a compact invariant torus. However, we prove that periodic solutions of $\alpha_2(t)$ are generically obstructed by a resonance mechanism, leading instead to an aperiodic but non-chaotic evolution. In this regime the invariant surface is non-compact and extends along the time direction, forming a *tube* rather than a torus. We therefore propose the term *tube integrability* for integrable systems whose invariant manifolds are non-compact in time. A perturbation expansion for $\alpha_2(t)$ up to third order is derived and compared with numerical integration, clarifying the parameter regimes in which the truncated series provides quantitatively accurate approximations. The breakdown of the series for small y_0 is shown to reflect the asymptotic nature of the expansion rather than a loss of integrability.

Keywords: nonlinear oscillators; time-dependent Hamiltonian systems; tube integrability; Ermakov–Lewis invariant; non-compact invariant manifolds; asymptotic expansions; resonance obstruction.

1 Introduction

Classical Liouville integrability is commonly associated with the geometry of invariant tori in phase space [7]. In this classical setting, compactness is essential: it permits the introduction of globally defined angle variables and ensures recurrent motion. When a system is explicitly time-dependent, however, the connection between integrability and compact invariant geometry no longer follows.

In this work we study the nonlinear oscillator

$$z'' + \omega^2 z + g(t)z^2 = 0 \quad (1.1)$$

where $g(t)$ varies smoothly in time. We show that this system admits an exact quadratic invariant $I(z, p, t)$, structurally related to the Ermakov–Lewis framework for time-dependent oscillators [2, 3, 4]. The existence of this invariant confines solutions to a smooth two-dimensional surface in the extended phase space (z, p, t) .

If $\alpha_2(t)$ is periodic, Floquet theory implies that these invariant surfaces form compact tori [6, 5]. However, we prove that periodic solutions of $\alpha_2(t)$ are generically obstructed by a second-order resonance mechanism, analogous to small-divisor effects in classical perturbation theory and averaging methods [13, 11]. As a consequence, the generic behavior of $\alpha_2(t)$ is aperiodic.

In this non-periodic regime the invariant surface does not close on itself, but forms a smooth, non-compact structure extending along the time axis. We therefore propose the term *tube integrability* to describe integrable systems whose invariant manifolds are non-compact in time.

The perturbation series for $\alpha_2(t)$ is shown to be asymptotic rather than convergent, with the eventual breakdown of truncations governed by nearby complex singularities in the continuation parameter [8, 9, 10]. This breakdown does not indicate a loss of integrability, but marks the natural limit of the truncated series.

Remark. The conceptual motivation for this work originates in the long-standing question of whether integrability is intrinsically tied to compact invariant geometry. The results presented here demonstrate that this need not be the case: exact integrability may coexist with non-compact invariant manifolds, provided the geometric structure is coherent and the invariant is global.

2 General formulation and derivation of the invariant

We start from the quadratic ansatz for a first integral

$$I(z, p, t) = a_0(z, t) + a_1(z, t)p + a_2(t)p^2, \quad p = z', \quad (2.1)$$

which was derived in [1] by requiring $\frac{dI}{dt} = 0$ for all trajectories of

$$z'' + \omega^2 z + g(t)z^2 = 0. \quad (2.2)$$

As shown previously, the general solution for the coefficient functions is

$$a_2(t) = \alpha_2(t), \quad (2.3)$$

$$a_1(z, t) = -\alpha'_2(t)z + \alpha_1(t), \quad (2.4)$$

$$a_0(z, t) = \omega^2 \alpha_2(t)z^2 + \frac{2}{3} \alpha_2(t)g(t)z^3 - \alpha'_1(t)z + \frac{1}{2} \alpha''_2(t)z^2 + \alpha_0(t). \quad (2.5)$$

Inserting these expressions into the determining equations yields the following coupled system:

$$\alpha''_1 + \omega^2 \alpha_1 = 0, \quad (2.1)$$

$$\alpha'''_2 + 4\omega^2 \alpha'_2 - 2\alpha_1 g(t) = 0, \quad (2.2)$$

$$5g(t)\alpha'_2 + 2\alpha_2 g'(t) = 0, \quad (2.3)$$

$$g(t) = \alpha_2(t)^{-5/2}. \quad (2.4)$$

Equation (2.1) admits the oscillatory solution

$$\alpha_1(t) = \frac{1}{2}C_1 \cos(\omega t) + \frac{1}{2}C_2 \sin(\omega t), \quad (2.5)$$

so that substitution into (2.2) yields the nonlinear third-order ODE

$$\alpha'''_2 + 4\omega^2 \alpha'_2 - [C_1 \cos(\omega t) + C_2 \sin(\omega t)] \alpha_2^{-5/2} = 0. \quad (2.6)$$

Taken together, (2.1)–(2.4) form the set of conditions for integrability in the quadratic case with nonzero $\alpha_1(t)$.

Finally, the quadratic invariant takes the explicit form

$$\begin{aligned} I(z, p, t) &= \alpha_2(t)p^2 - \alpha'_2(t)zp + \alpha_1(t)p \\ &+ \left(\omega^2 \alpha_2(t) + \frac{1}{2} \alpha''_2(t) \right) z^2 - \alpha'_1(t)z + \frac{2}{3} \alpha_2(t)g(t)z^3 = K. \end{aligned} \quad (2.7)$$

Summary of the integrable system:

$$(S1) \ z'' + \omega^2 z + g(t)z^2 = 0$$

$$(S2) \ g(t) = \alpha_2(t)^{-5/2}$$

$$(S3) \ \alpha_2''' + 4\omega^2\alpha_2' - [C_1 \cos(\omega t) + C_2 \sin(\omega t)] \alpha_2^{-5/2} = 0$$

$$(S4) \ I(z, p, t) = \alpha_2(t)p^2 - \alpha_2'(t)zp + \alpha_1(t)p \\ + \left(\omega^2\alpha_2(t) + \frac{1}{2}\alpha_2''(t) \right) z^2 - \alpha_1'(t)z + \frac{2}{3}\alpha_2(t)g(t)z^3 = K$$

3 Tube integrability

From Eqs. (S3) and (S4) we see, that periodic solutions of $\alpha_2(t)$ lead to classical invariant tori in the extended phase space while non-periodic solutions require a different concept. In this general case we introduce the notion of *tube integrability* which extends the classical concept of Liouville integrability to certain non-periodic situations.

Definition 3.1 (Tube integrability). We denote a system

$$z'' + \omega^2 z + g(t) z^2 = 0$$

as *tube integrable* if there exists a polynomial invariant

$$I(z, p, t) = \sum_{k=0}^N a_k(t) p^k, \quad p = z',$$

with smooth time-dependent coefficients $a_k(t)$, such that $\frac{d}{dt}I(z(t), p(t), t) \equiv 0$, even though the coefficient functions $a_k(t)$ are not periodic in t .

In this case, the flow $(z(t), p(t), t)$ is restricted to a smooth two-dimensional invariant surface in the extended phase space (z, p, t) . Since $a_k(t)$ are not periodic, a Poincaré section at times $t = nT$ is formally admissible but does not produce closed invariant curves in the (z, p) -plane. Instead, the motion is confined to an *invariant tube*, a non-periodic deformation of a classical invariant torus.

Tube integrability (B/W): aperiodic tube with wrapping orbit

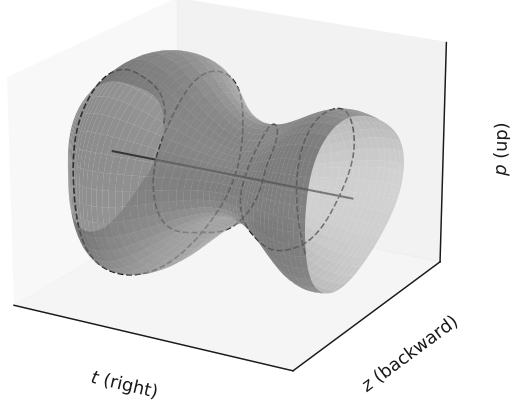


Figure 1: Schematic illustration of tube integrability. The t -axis (right) runs inside the tube, while the cross-section (z, p) varies aperiodically so that no invariant torus arises. Instead, the solution winds around the t -axis on a non-periodic tube surface.

Note that tube integrability is a property of the original z -equation (1.1). The auxiliary function $y(\tau) = \alpha_2(t)$ appears only through the time-dependent coefficient $g(t) = y^{-5/2}$ which determines the geometry of the invariant surface. Thus, periodic y would imply torus integrability of the z -equation, while aperiodic y yields tube integrability of the z -equation.

Remark 3.1. Classical Liouville integrability with periodic coefficients $a_k(t)$ leads to invariant two-dimensional tori in the extended phase space and to closed invariant curves in Poincaré sections. In contrast, tube integrability describes the situation where the invariant surface is topologically a “tube” rather than a torus: the trajectory winds quasiperiodically or even irregularly along the time direction, without closing. From the point of view of (z, p) only, the motion therefore appears irregular and does not admit classical Poincaré invariant curves, even though an exact invariant $I(z, p, t)$ still exists. Consequently, the lack of periodicity in $\alpha_2(t)$ is directly transferred to the z -equation: no invariant tori arise, but the invariant surfaces are of tube type.

As an explicit illustration of tube integrability, we present in Fig. 2 a numerical example with nonperiodic $\alpha_2(t)$. The four panels display $\alpha_2(t)$,

the corresponding coefficient $g(t) = \alpha_2(t)^{-5/2}$, the resulting solution $z(t)$, and the quadratic invariant $I(t)$.

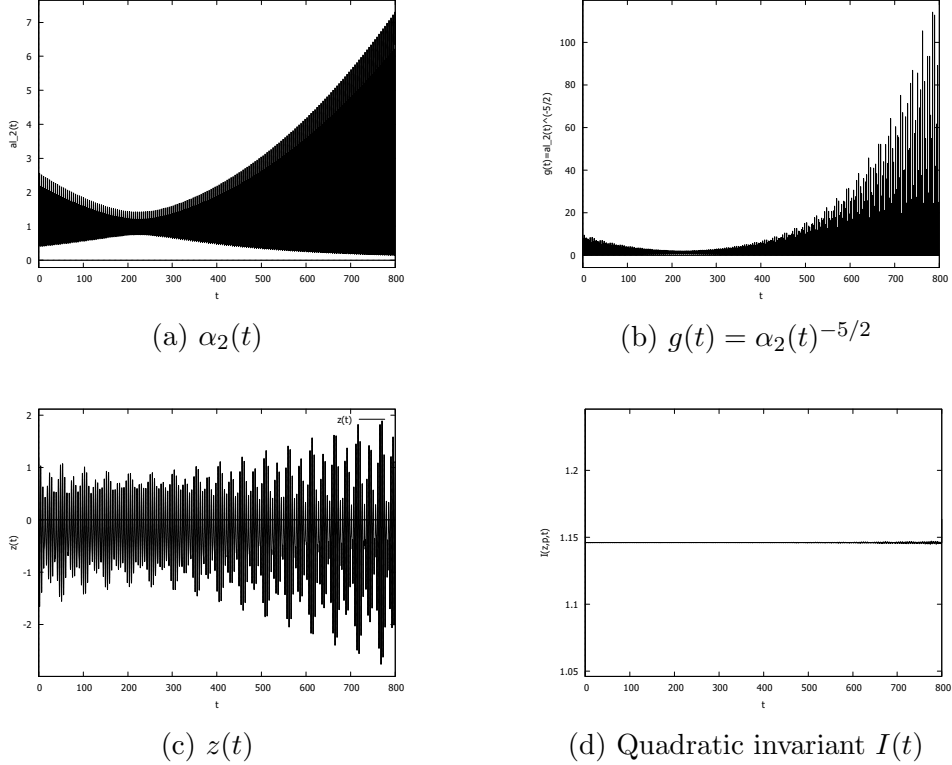


Figure 2: Illustration of *tube integrability* in the case of a nonperiodic $\alpha_2(t)$. The function $\alpha_2(t)$ shows dominant frequencies ω and 2ω together with a slowly modulated envelope. The coefficient $g(t)$ injects energy, leading to irregular but bounded oscillations of $z(t)$. Nevertheless the quadratic invariant $I(t)$ remains conserved up to numerical accuracy, confirming motion on an invariant tube.

3.1 Example: tube integrability via the Ermakov–Pinney construction

As an illustrating example of tube integrability in the sense of the above definition, we consider the linear oscillator

$$z'' + f(t)z = 0, \quad (3.1)$$

and let $w(t)$ be any strictly positive solution of the Ermakov–Pinney equation

$$w'' + f(t) w = \frac{1}{w^3}. \quad (3.2)$$

Then the Lewis–Ermakov invariant

$$I(z, p, t) = \frac{1}{2} \left(\left(\frac{z}{w} \right)^2 + (w p - w' z)^2 \right), \quad p = z', \quad (3.3)$$

satisfies $\frac{d}{dt} I(z(t), p(t), t) \equiv 0$ along all solutions of (3.1), for *any* given coefficient $f(t)$.

Sketch. A direct differentiation of (3.3) and substitution of $z'' = -f(t)z$ and $w'' = -f(t)w + 1/w^3$ yields $\dot{I} \equiv 0$. \square

Tube (vs. torus) behavior. If $f(t)$ is T –periodic, the coefficients in (3.3) are T –periodic and classical Liouville integrability manifests in invariant tori (closed invariant curves in Poincaré sections). If, however, $f(t)$ is nonperiodic—e.g. obtained from a chaotic driver—then I still defines an exact invariant surface in the extended space (z, p, t) , but the surface winds nonperiodically in t , hence an *invariant tube* rather than a torus; classical Poincaré sections in (z, p) do not yield closed invariant curves.

Chaotic forcing example (logistic driver). Let $\{\ell_n\}$ be the logistic map at $\mu = 4$, $\ell_{n+1} = 4\ell_n(1 - \ell_n)$ on $[0, 1]$. Choose a sampling period $T_s > 0$ and define a smooth C^2 interpolation $\tilde{f}(t)$ such that $\tilde{f}(nT_s) = f_0 + \Delta f (2\ell_n - 1)$ for parameters $f_0 > 0$, $\Delta f \in (0, f_0)$. (For instance, use cubic splines on the grid $t = nT_s$.) Set $f(t) = \tilde{f}(t)$ in (3.1)–(3.2). Then $f(t)$ is aperiodic (chaotic in the sense of the underlying symbolic dynamics), while the invariant (3.3) remains exact. Consequently, the motion of (3.1) is confined to an invariant tube defined by $I = \text{const}$, i.e. the system is *tube integrable*.

4 Properties and computation of the function $\alpha_2(t)$

As has been shown in section 2, the function $\alpha_2(t)$ given by the third order nonlinear differential equation (S3) via its solutions generates an infinite number of integrable systems for the associated z equation (1.1). In this section we discuss the properties of $\alpha_2(t)$ as well as perturbative approaches to this explicitly time dependent nonlinear equation.

4.1 Transformation of the independent variable

We first rewrite the dependent variable α_2 replacing it by y and start from the original equation

$$y''' + 4\omega^2 y' - [C_1 \cos \omega t + C_2 \sin \omega t] y^{-\frac{5}{2}} = 0 \quad (4.1)$$

Next, we simplify the equation, rescaling the independent variable as

$$\tau = \omega t \quad (4.2)$$

leading to

$$y''' + 4y' - \frac{1}{\omega^3} [C_1 \cos \tau + C_2 \sin \tau] y^{-\frac{5}{2}} = 0 \quad (4.3)$$

where from this point ' denotes the derivative w.r.t. τ . We consider all the variables and constants included in (4.3) to be real numbers.

4.2 Positivity of $y(\tau)$

We prove the important Lemma:

Lemma: All solutions of (4.3) are strictly positive functions, $y(\tau) > 0$

Proof by contradiction: We rewrite (4.3) as

$$y''' + 4y' = \frac{1}{\omega^3} [C_1 \cos \tau + C_2 \sin \tau] y^{-\frac{5}{2}} \quad (4.4)$$

Let's consider the existance of an interval (τ_1, τ_2) in which $y < 0$. Then the left side of the above equation remains a real function. However, the right hand side of the equation, due to the power $-\frac{5}{2}$, becomes a pure imaginary function which makes it impossible to satisfy the differential equation. In order to avoid the contradiction, we conclude $y > 0$ for all possible solutions of (4.3). q.e.d.

4.3 Reduction of the non autonomous term to a single cosine function

Since the nonautonomous part of (4.3) can be written as a cosine function in the form:

$$C_1 \cos \tau + C_2 \sin \tau = \sqrt{C_1^2 + C_2^2} \cos(\tau - \Phi) \quad (4.5)$$

we may, without loss of generality, rewrite the y-equation as

$$y''' + 4y' = \varepsilon \cos \tau y^{-\frac{5}{2}} \quad (4.6)$$

by using

$$\varepsilon = \frac{C}{\omega^3} ; \quad C = \sqrt{C_1^2 + C_2^2} \quad (4.7)$$

as well as applying a linear constant shift of Φ to the independent variable.

4.4 Concerning the existence of a periodic solution for $y(\tau)$

We now address the question whether the function $y(\tau)$ can admit strictly periodic solutions. As has been shown, $y(\tau)$ satisfies

$$y''' + 4y' + \varepsilon y^{-5/2} \cos \tau = 0, \quad y(\tau) = \alpha_2(t), \quad \varepsilon = \frac{C}{\omega^3}, \quad (4.8)$$

with $\tau = \omega t$.

Proposition 4.1 (Non-existence of small 2π -periodic solutions). Let $m > 0$ and suppose that $y(\tau) = \alpha_2(t)$ is a 2π -periodic solution of (4.8) with mean value

$$m = \frac{1}{2\pi} \int_0^{2\pi} y(\tau) d\tau.$$

Then for $\varepsilon \neq 0$ and $C_1 \neq 0$ no such solution bifurcates from the constant state $y \equiv m$.

Sketch of proof. Write $y(\tau) = m + u(\tau)$ with $\int_0^{2\pi} u(\tau) d\tau = 0$. Linearization gives the operator $L = D^3 + 4D$ on 2π -periodic functions, with kernel

$$\ker L = \text{span}\{1, \sin(2\tau), \cos(2\tau)\}.$$

At order $\mathcal{O}(\varepsilon)$ one finds a 2π -periodic correction $u_1(\tau) = a_1 \sin \tau$. At order $\mathcal{O}(\varepsilon^2)$, however, the nonlinear expansion of $y^{-5/2}$ generates a forcing proportional to $\sin(2\tau)$, which lies inside $\ker L$. By Fredholm's alternative, solvability requires this resonant component to vanish, but its coefficient $\propto \varepsilon^2 m^{-6}$ is nonzero for $\varepsilon \neq 0$. Hence the solvability condition fails and no small 2π -periodic solution can exist near $y \equiv m$. \square

Remark 4.1. The resonance obstruction is fundamental. Since the forcing $\cos \tau$ fixes the external frequency, Poincaré–Lindstedt detuning is not available in this non-autonomous setting. The consequences are:

- Up to first order in ε one finds a strictly 2π -periodic approximation of $\alpha_2(t)$, so the solution appears “almost periodic” on short time scales.
- At second order the resonant $\sin(2\tau)$ contribution produces unavoidable secular terms, destroying exact periodicity.
- For $C_1 = 0$ the constant solution remains valid. For $C_1 \neq 0$, $\alpha_2(t)$ is never exactly 2π -periodic: it is at best *almost periodic*, but in fact genuinely aperiodic.
- As a consequence, the invariant $I(z, p, t)$ of the z -equation still exists, but induces only *tube integrability* in the extended phase space (z, p, t) , not a genuine invariant torus.

4.5 Fourier expansion and resonance mechanism

For completeness we display the Fourier system corresponding to equation (4.8). We expand

$$y(\tau) = c_0 + \sum_{n \geq 1} (c_n \cos(n\tau) + s_n \sin(n\tau)), \quad (4.9)$$

with $c_0 > 0$ the mean value.

4.5.1 First order

At order $\mathcal{O}(\varepsilon)$ one obtains

$$s_1 = -\frac{\varepsilon}{3} c_0^{-5/2}, \quad c_n = s_n = 0 \quad (n \geq 2).$$

Thus the first correction is purely $\sin \tau$, consistent with the forcing phase.

4.5.2 Second order

Expanding $y^{-5/2}$ produces quadratic terms of the form

$$(c_0 + s_1 \sin \tau)^{-5/2} = c_0^{-5/2} \left(1 - \frac{5}{2} \frac{s_1}{c_0} \sin \tau + \frac{35}{8} \frac{s_1^2}{c_0^2} \sin^2 \tau + \dots \right).$$

The $\sin^2 \tau$ term generates a second harmonic $\propto \sin(2\tau)$ with coefficient

$$-\frac{5}{96} \varepsilon^2 c_0^{-6}.$$

Since $(D^3 + 4D)(\sin 2\tau) = 0$, this contribution lies in the kernel of the linear operator and produces a secular term $\propto \tau \sin(2\tau)$. This illustrates explicitly why the Fourier system has no consistent 2π -periodic solution at order ε^2 .

4.5.3 Third order

For completeness, the cubic term forces a third harmonic

$$s_3 = -\frac{7}{864} \varepsilon^3 c_0^{-19/2}, \quad c_3 = 0.$$

Higher harmonics can in principle be computed recursively, but the inconsistency at order ε^2 already prevents exact periodicity.

In summary, the Fourier system (4.9) confirms the Proposition 4.1: the unavoidable $\sin(2\tau)$ forcing at second order makes the system unsolvable in the class of 2π -periodic functions. The apparent periodicity at first order is destroyed by resonance at higher order.

5 Perturbation theoretic computation of $y(\tau)$

Since (4.6) is a nonlinear, explicitly time dependent differential equation of order 3, we may not expect to find closed analytical expressions to its solutions. It is for this reason, that we introduce a perturbative treatment in order to approach the equations behaviour in an analytical way. It turned out however, that we are left with simpler expressions if we first integrate the entire equation w.r.t. τ , leading to a volterra type integro-differential equation:

$$y''(\tau) + 4y(\tau) = y_0'' + 4y_0 + \varepsilon \int_0^\tau y(s)^{-5/2} \cos s ds, \quad (5.1)$$

As can be seen the solution of this equation depends on 4 free parameters, namely the initial conditions y_0, y_0' and y_0'' as well as on the parameter ε defining the strength of the nonlinear contribution in the integrand. However, in order to keep the computations straightforward as possible, we set $y_0' =$

$y_0'' = 0$ and remain with just two independent parameters y_0 and ε . Under this restriction (5.1) reduces to

$$y'' + 4y = 4y_0 + \varepsilon \int_0^\tau y(s)^{-\frac{5}{2}} \cos s ds \quad (5.2)$$

Next we take care of the fact that $y(\tau)$ for all real values of the independent variable. In order to keep this property for the entire perturbation procedure, we use the substitution:

$$y(\tau) = e^{\rho(\tau)} \quad (5.3)$$

Under this substitution we get

$$y' = y\rho'; y'' = y'\rho' + y\rho'' = y\rho'^2 + y\rho'' \quad (5.4)$$

Inserting the so obtained substitutions into (5.2) and dividing by e^ρ gives the new integro-differential equation for $\rho(\tau)$ as:

$$\rho'' + (\rho')^2 + 4 = 4y_0 e^{-\rho} + \varepsilon e^{-\rho} \int_0^\tau e^{-5\rho(s)/2} \cos s ds. \quad (5.5)$$

We aim for a perturbation expansion up to ε^2 , hence we let:

$$\rho(\tau) = \rho_0 + \varepsilon \rho_1(\tau) + \varepsilon \rho_2(\tau) + \mathcal{O}(\varepsilon^3) \quad (5.6)$$

Order $\mathcal{O}(1)$

Comparing terms independent of ε from (5.5) we get $4 = 4y_0 e^{-\rho_0}$, hence

$$\boxed{\rho_0 = \ln y_0.} \quad (5.7)$$

Order $\mathcal{O}(\varepsilon)$

Collecting $\mathcal{O}(\varepsilon)$ -terms gives

$$\rho_1'' + 4\rho_1 = y_0^{-7/2} \sin \tau, \quad \rho_1(0) = \rho_1'(0) = 0, \quad (5.8)$$

so that

$$\boxed{\rho_1(\tau) = y_0^{-7/2} \left(\frac{1}{3} \sin \tau - \frac{1}{6} \sin 2\tau \right).} \quad (5.9)$$

Order $\mathcal{O}(\varepsilon^2)$

At second order one finds

$$\begin{aligned} \rho_2'' + 4\rho_2 &= 2\rho_1^2 - (\rho_1')^2 + y_0^{-7/2} \left[-\frac{5}{2} \int_0^\tau \rho_1(s) \cos s \, ds - \rho_1(\tau) \sin \tau \right], \quad (5.10) \\ \rho_2(0) &= \rho_2'(0) = 0. \end{aligned}$$

Inserting (5.9) and evaluating the elementary integrals yields the explicit solution

$$\begin{aligned} \rho_2(\tau) &= y_0^{-7} \left[-\frac{5}{288} - \frac{1}{24} \cos \tau + \frac{19}{288} \cos 2\tau - \frac{1}{72} \cos 3\tau \right. \\ &\quad \left. + \frac{1}{144} \cos 4\tau + \frac{5}{96} \tau \sin 2\tau \right]. \end{aligned} \quad (5.11)$$

The term $\frac{5}{96}y_0^{-7}\tau \sin(2\tau)$ encodes the intrinsic second-order secular response at the 2:1 resonance.

Composite $\mathcal{O}(\varepsilon^2)$ approximation for $y(\tau)$

Expanding e^ρ to second order gives

$$y(\tau) = e^{\rho(\tau)} = y_0 \left[1 + \varepsilon \rho_1(\tau) + \varepsilon^2 \left(\rho_2(\tau) + \frac{1}{2} \rho_1(\tau)^2 \right) \right] + \mathcal{O}(\varepsilon^3), \quad (5.12)$$

with ρ_1, ρ_2 from (5.9)–(5.11).

Scaling remark. Writing $y(\tau) = y_0 \tilde{y}(\tau)$ and normalizing (5.1) shows that the effective small parameter is

$$\varepsilon_{\text{eff}} = \varepsilon y_0^{-7/2},$$

which explains the strong improvement of accuracy for larger y_0 and the deterioration for $y_0 \ll 1$.

Heuristic validity window. The dominant secular piece in (5.12) scales like $\sim \frac{5}{96} \varepsilon^2 y_0^{-6} \tau \sin(2\tau)$. A practical criterion is therefore

$$\tau < \tau^* = \frac{96y_0^6}{5\varepsilon^2} \quad (5.13)$$

5.1 Third-order contribution $\rho_3(\tau)$

We recall the Volterra formulation

$$\rho''(\tau) + 4\rho(\tau) = -\frac{5}{2}\varepsilon e^{-\frac{5}{2}\rho(\tau)} \int_0^\tau e^{-\frac{5}{2}\rho(s)} \cos s ds, \quad (5.14)$$

with $\rho(0) = \rho'(0) = 0$. Expanding $\rho(\tau) = \sum_{n \geq 1} \varepsilon^n \rho_n(\tau)$ and the RHS of ((5.5)) up to order ε^3 yields

$$\rho_3''(\tau) + 4\rho_3(\tau) = F_3(\tau), \quad (5.15)$$

where the source term is

$$\begin{aligned} F_3(\tau) = & -\frac{5}{2}e^{-\frac{5}{2}\rho_0} \left[-\frac{5}{2}\rho_2(\tau) + \frac{25}{8}\rho_1(\tau)^2 \right] \int_0^\tau e^{-\frac{5}{2}\rho_0} \cos s ds \\ & - \frac{5}{2}e^{-\frac{5}{2}\rho_0} \int_0^\tau \left[-\frac{5}{2}\rho_2(s) + \frac{25}{8}\rho_1(s)^2 \right] e^{-\frac{5}{2}\rho_0} \cos s ds. \end{aligned} \quad (5.16)$$

Here ρ_1 and ρ_2 are the previously obtained first and second order solutions. The inhomogeneous equation for with initial data $\rho_3(0) = \rho_3'(0) = 0$ can easily be solved by comparing the coefficients of all trigonometric functions and of the appearing resonance terms. Finally we obtain:

$$\begin{aligned} \rho_3(\tau) = & \frac{1}{2592 y_0^{21/2}} \left[-\frac{45}{4}\tau + \frac{135}{4}\tau \cos \tau - \frac{45}{2}\tau \cos(2\tau) + \frac{45}{4}\tau \cos(3\tau) \right. \\ & - \frac{45}{4}\tau \cos(4\tau) + \frac{159}{2}\sin \tau - \frac{327}{4}\sin(2\tau) + \frac{73}{4}\sin(3\tau) + \frac{69}{8}\sin(4\tau) \\ & \left. - \frac{9}{4}\sin(5\tau) + \sin(6\tau) \right]. \end{aligned} \quad (5.17)$$

5.2 Comparison of the perturbation results to numeric integration

As a first example we use the parameters $\varepsilon = 0.1$ and $y_0 = 1$ and compare the analytical and numerical solutions in the interval $400 < \tau < 500$. While the numerical results have been obtained by use of a Runge-Kutta 4 integration

of (4.6), the analytical result comes from evaluating the above perturbation theoretic computations to third order in ε . Visualisation of the results has been restricted to the end of the integration interval, since in this region we expect the largest differences between analysis and numeric integration. However, we observe a perfect agreement between the analytical (red) and numerical solutions (green), which is consistent with (5.13) , leading to a range of validity of $\tau_* < 1920$ which lies far above the integration interval of $\tau = [0, 500]$. In Fig. 3 we plot the numeric solution (red) together with the perturbation theoretic result (green).

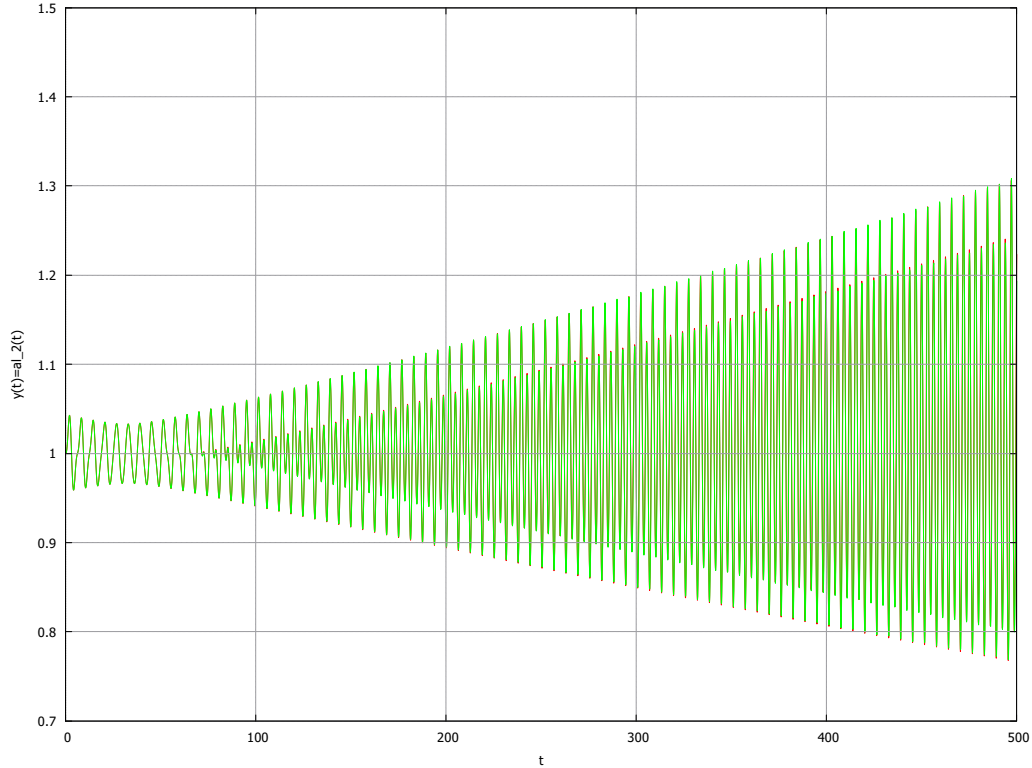


Figure 3: Numeric versus analytic solution of (4.6) for $y_0 = 1$, $\varepsilon = 0.1$.

As can be seen, we have an excellent agreement of the analytical result and the numerical integration for $y_0 = 1$ and $\varepsilon = 0.1$. This is consistent with the theoretical validity region computed in (5.13) which reaches up to $\tau_* = 1920$, well above the integration interval used. However, decreasing y_0 to 0.7 the agreement between numerical and analytic computations starts to become less accurate. In the first interval $0 < t < 300$ shown in Fig. 4 the agreement is still reasonable up to about $\tau = 200$, the theoretical limit being

$\tau_* = 225$. Above this limit the functions start to differ significantly. This becomes clearly visible in Fig. 5 where the numeric and analytic solutions differ by nearly 50% at $\tau = 500$.

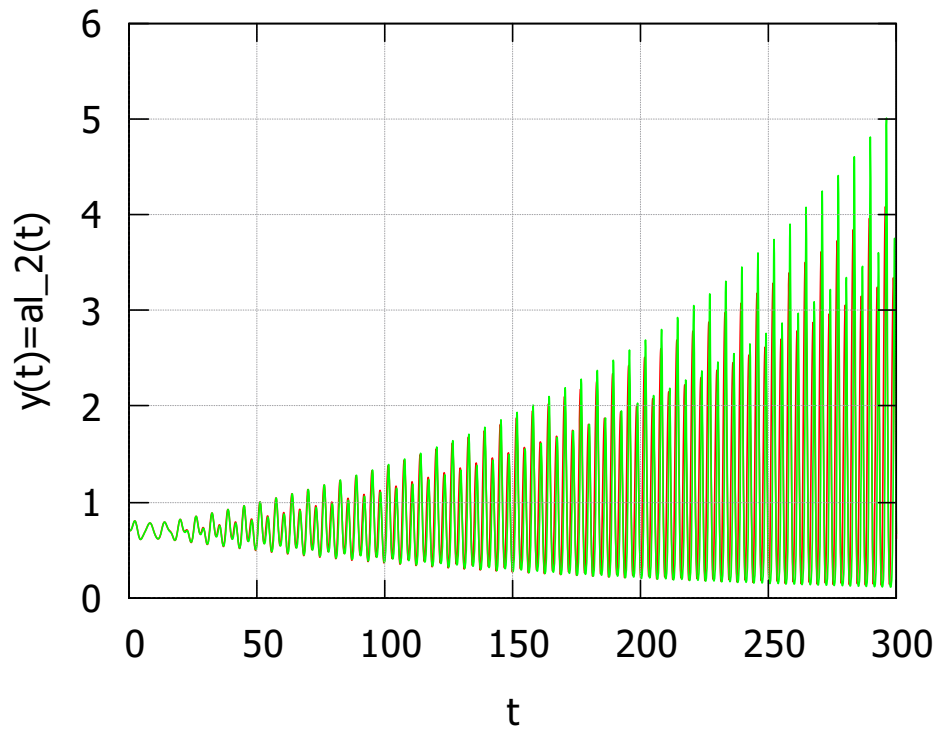


Figure 4: Numeric versus analytic solution when $y_0 = 0.7$, $\varepsilon = 0.1$ and $0 < t < 300$

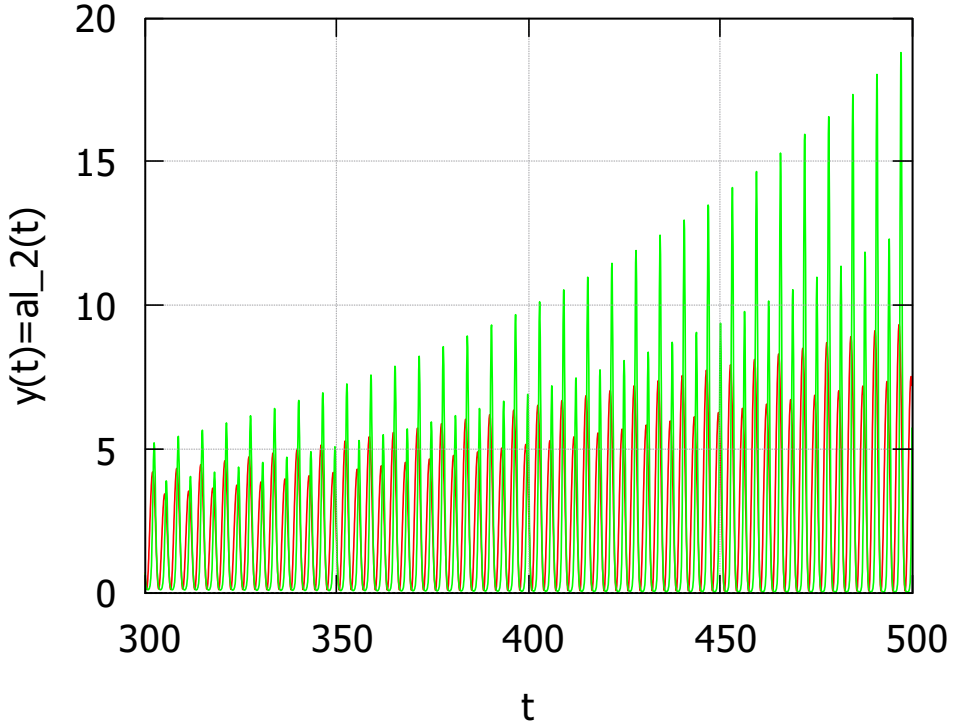


Figure 5: Numeric versus analytic solution when $y_0 = 0.7$, $\varepsilon = 0.1$ and $300 < t < 500$

Note that for all graphs, the positivity property of y is still strictly preserved due to consequently keeping the ansatz $y = e^{\rho(\tau)}$ throughout the computations.

In conclusion, the good agreement between the analytical and numerical results within the predicted interval $\tau < \tau_*$ provides a clear confirmation of criterion (5.13). The perturbative expansion up to $\mathcal{O}(\varepsilon^3)$ accurately reproduces the dynamics of (4.6) as long as the secular term remains sufficiently small, while the onset of deviation beyond τ_* marks the natural limit of the perturbative validity. This demonstrates that the analytical approach not only captures the qualitative structure of $y(\tau)$ but also yields quantitatively reliable results within its theoretical window of applicability.

6 Evaluation of the results

In order to keep the analytic expressions simple as possible, for the evaluation of results we will restrict to the case $\omega = 1$. In this case $\tau = t$ and $C_1 = \varepsilon$. As before we keep $C_2 = 0$. So we inspect the invariant I related to

$$z'' + z + g(t)z^2 = 0 ; \quad g(t) = \alpha_2(t)^{-\frac{5}{2}} \quad (6.1)$$

In the following subsection we compute the analytical expression for the invariant I based on the perturbation expansion of $\alpha_2(t) = y(t)$ to third order in ε :

$$\alpha_2(t) = y_0 e^{\varepsilon \rho_1(t) + \varepsilon^2 \rho_2(t) + \varepsilon^3 \rho_3(t) + O(\varepsilon^4)} \quad (6.2)$$

6.1 Analytical approximation of the invariant $I(z, p, t)$

We start from the invariant as given in (S4) with $\omega = 1$, $C_1 = \varepsilon$ and $C_2 = 0$.

$$\begin{aligned} I(z, p, t) = & \alpha_2(t)p^2 - \alpha'_2(t)zp + \alpha_1(t)p + \left(\alpha_2(t) + \frac{1}{2}\alpha''_2(t) \right)z^2 \\ & - \alpha'_1(t)z + \frac{2}{3}\alpha_2(t)g(t)z^3 = K \end{aligned} \quad (6.3)$$

From the perturbative treatment:

$$\alpha_2(t) = y_0 e^{\varepsilon \rho_1(t) + \varepsilon^2 \rho_2(t) + \varepsilon^3 \rho_3(t)} \quad (6.4)$$

follows

$$\alpha'_2(t) = \alpha_2(t) (\varepsilon \rho'_1(t) + \varepsilon^2 \rho'_2(t) + \varepsilon^3 \rho'_3(t)) \quad (6.5)$$

In principle we could derive $\alpha''_2(t)$ from $\alpha'(t)$ by direct differentiation but this would generate an inaccuracy due to amplification of numerical errors in truncated expansions while differentiating. Instead we derive $\alpha''_2(t)$ directly from the Volterra equation (5.2) and get

$$\alpha''_2(t) = 4[y_0 - \alpha_2(t)] + \varepsilon \int_0^t \alpha_2(s)^{-\frac{5}{2}} \cos s ds \quad (6.6)$$

Using this method we replace differentiation of truncated expressions by integration which avoids numerical error amplification. Expanding the integrand w.r.t. ε finally the invariant (6.3) is given by:

$$I(z, p, t) = A_1(t)z + A_2(t)p + A_3(t)z^2 + A_4(t)zp + A_5(t)p^2 + A_6(t)z^3 \quad (6.7)$$

with

$$A_1(t) = -\alpha'_1(t) = -\frac{1}{2}\varepsilon \sin t \quad (6.8)$$

$$A_2(t) = \alpha_1(t) = \frac{1}{2}\varepsilon \cos t \quad (6.9)$$

$$A_3(t) = \alpha_2(t) + \frac{1}{2}\alpha''_2(t) = A_{31}(t) + y_0 e^{A_{32}(t)} \quad (6.10)$$

where

$$\begin{aligned} A_{31}(t) &= \frac{\varepsilon^3}{6912y_0^2} (-25 \sin 5t + 120 \sin 4t - 531 \sin 3t + 644 \sin 2t \\ &\quad - 230 \sin t + 135t \cos 3t + 120t \cos 2t - 75t \cos t) \\ &\quad + \frac{\varepsilon^2}{144y_0^6} (-9 \cos 3t + 4 \cos 2t + 5 \cos t) + \frac{\varepsilon}{6y_0^{\frac{5}{2}}} (2 \sin 2t - \sin t) \end{aligned} \quad (6.11)$$

$$\begin{aligned} A_{32}(t) &= \frac{\varepsilon^3}{2592y_0^{\frac{21}{2}}} \left(\sin 6t - \frac{9}{4} \sin 5t + \frac{69}{8} \sin 4t + \frac{73}{4} \sin 3t - \frac{327}{4} \sin 2t + \right. \\ &\quad \left. \frac{159}{2} \sin t - \frac{45}{4}t \cos 4t + \frac{45}{4}t \cos 3t - \frac{45}{2}t \cos 2t + \frac{135}{4}t \cos t - \frac{45}{4}t \right) \\ &\quad + \frac{\varepsilon^2}{y_0^7} \left(\frac{1}{144} \cos 4t - \frac{1}{72} \cos 3t + \frac{19}{288} \cos 2t - \frac{1}{24} \cos t \right) \\ c &\quad + \frac{5}{96}t \sin 2t - \frac{5}{288} \left(\frac{1}{3} \sin t - \frac{1}{6} \sin 2t \right) \end{aligned} \quad (6.12)$$

$$\begin{aligned} A_4(t) &= -\frac{\varepsilon^3}{3456y_0^{\frac{19}{2}}} (5 \cos 5t - 30 \cos 4t + 192 \cos 3t - 292 \cos 2t + 155 \cos t \\ &\quad + 45t \sin 3t + 60t \sin 2t - 75t \sin t - 30) \\ &\quad - \frac{\varepsilon^2}{288y_0^6} (-12 \sin 3t - 7 \sin 2t + 20 \sin t + 30t \cos 2t) \\ &\quad + \frac{\varepsilon}{3y_0^{\frac{5}{2}}} (\cos t - \cos 2t) \end{aligned} \quad (6.13)$$

$$A_5(t) = \alpha_2(t) = y_0 e^{\rho(t)} = y_0 e^{\rho(t)} \quad (6.14)$$

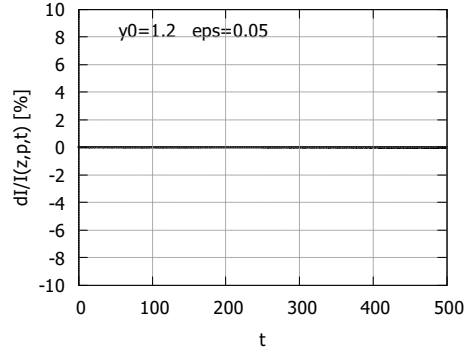
with $\rho_n(t)$ given in (5.9) - (5.17).

$$A_6(t) = \frac{2}{3} \alpha_2(t) g(t) = \frac{2}{3} \alpha_2(t)^{-\frac{3}{2}} = \frac{2}{3} y_0 e^{-\frac{3}{2}\rho(t)} \quad (6.15)$$

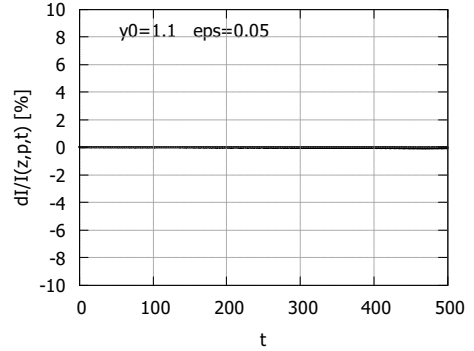
In order to check for the invariant property of (6.7) we numerically integrate the associated nonlinear equation (6.1) with initial conditions $z_0 = 0.2$, $z'(0) = p_0 = 0$. over the time interval $0 < t < 500$ and use the successive values at points $t_n = n\Delta t$ as well as t_n to be inserted into the analytic expression (6.7). We then compute the deviation (in %) from the initial value of $I(t)$. In theory this value should be equal to zero but due to the truncation of the perturbative solution, we expect a remaining time variation. We have two free parameters to our disposal, namely ε and y_0 , leading to coefficient functions $g_{\varepsilon, y_0}(t)$ entering (6.1). We fix $\varepsilon = 0.05$ and use four values for y_0 , namely $y_0 = 1.2, 1.1, 0.9, 0.8$. Inspecting the analytic expressions (5.9), (5.11) and (5.17) it becomes clear, that this behaviour arises from increasingly high powers of y_0 in the denominators of the perturbation contributions which attenuate high order perturbation contributions for $y_0 > 1$ as it strengthens them when $y_0 < 1$. Infact in the four figures below we observe the predicted behaviour. While for $y_0 > 1$ the invariant shows no visible variation (infact in the tenth of % regime) this changes abruptly as $y_0 < 1$, so that for $y_0 = 0.8$ the variation of the approximation reaches 8%.

It is important to mention, that these variations are not due to the fact of the integral itself just being valid locally, but only to a vanishing convergence of the perturbation series in the regime $y_0 < 1$!

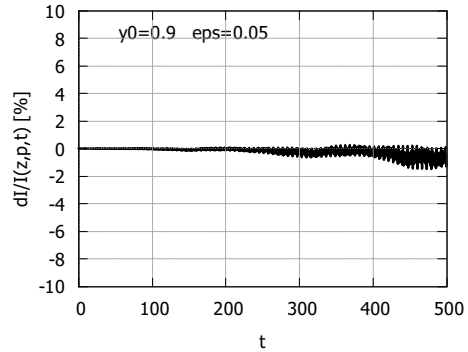
Finally we present a figure of the coefficient function $g(t) = \alpha_2(t)^{-\frac{5}{2}}$ rendering (6.1) integrable, using $y_0 = 1.1$ and $\varepsilon = 0.05$. For low values of t it behaves like a damped oscillation reaching an amplitude minimum and then starts growing indefinitely while exhibiting a superposition of alt least two frequencies ($T = \pi$ and 2π) with linearly increasing amplitude.



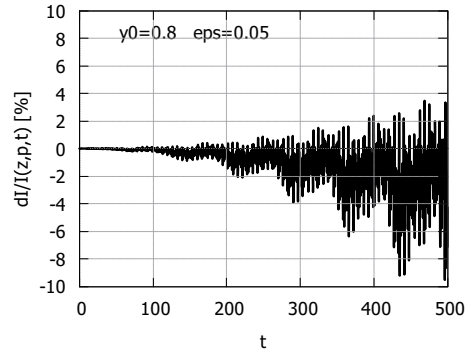
(a) $y_0 = 1.2$, $\epsilon = 0.05$ — no variations visible.



(b) $y_0 = 1.1$, $\epsilon = 0.05$ — very small variations visible.



(c) $y_0 = 0.9$, $\epsilon = 0.05$ — A variation of about 2% becomes visible



(d) $y_0 = 0.8$, $\epsilon = 0.05$ — A strong variation of 9% appears

Figure 6: Variations of the approximate analytical invariant $I(z, p, t)$ in percents of its initial value for $\epsilon = 0.05$ and $y_0 = 1.2, 1.1, 0.9, 0.8$

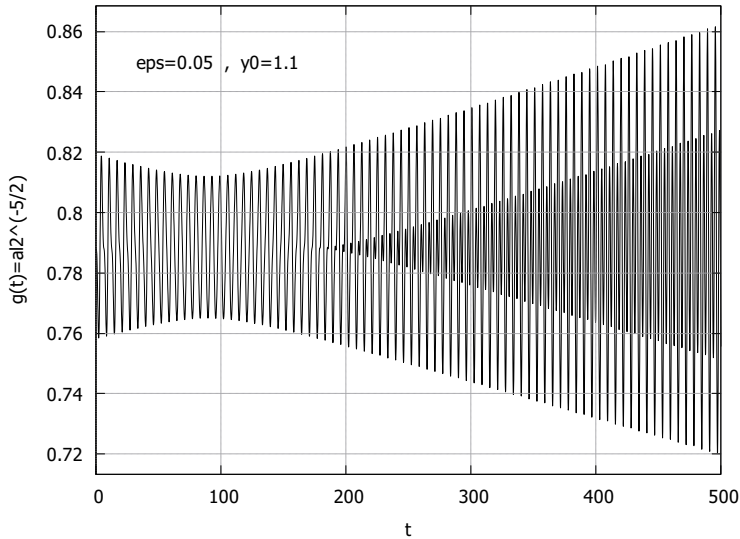


Figure 7: Graph of the coefficient function $g(t)$ when $\varepsilon = 0.05$ and $y_0 = 1.1$

7 Conclusions

We have analyzed the nonlinear oscillator (2.2) with a time-dependent coefficient $g(t)$ and shown that it admits an exact quadratic invariant provided that $g(t) = \alpha_2(t)^{-5/2}$ and $\alpha_2(t)$ satisfies the nonlinear third-order equation derived in Section 2. This establishes a broad class of integrable non-autonomous systems.

A central finding is the qualitative distinction between two geometric regimes. If $\alpha_2(t)$ is periodic, the invariant surfaces are compact and form invariant tori, recovering the classical Liouville picture. However, we have shown that periodic solutions of $\alpha_2(t)$ are generically obstructed by a second-order resonance mechanism, which enforces a slow but unavoidable aperiodic modulation. In this generic regime, the invariant surfaces become non-compact: the motion remains strictly confined, but the trajectory winds along a *tube* rather than closing on a torus.

We have proposed the term *tube integrability* to characterize this regime: the system retains a global invariant and regular geometric structure, but the associated invariant manifolds are non-compact in the time direction. This extends the conceptual scope of integrability beyond the classical assumption of compactness.

To understand the behavior of $\alpha_2(t)$ in the non-periodic setting, we developed a perturbation expansion up to third order and verified its accuracy against numerical integration. The effective small parameter was shown to be $\varepsilon_{\text{eff}} = \varepsilon y_0^{-7/2}$, explaining the transition between quantitatively stable and unstable approximation regimes.

Crucially, the breakdown of accuracy for $y_0 < 1$ does *not* indicate a loss of integrability. The invariant $I(z, p, t)$ remains exact for all t . What breaks down is only the truncated asymptotic expansion of $\alpha_2(t)$, whose coefficients are governed by nearby singularities in the complex ε -plane. Thus the observed drift of $I(z, p, t)$ in this regime reflects the natural limit of the perturbation series, not a transition to chaotic dynamics.

In summary, this work identifies and characterizes a coherent form of integrability beyond periodicity, in which the invariant structure is non-compact but fully regular. This raises several natural directions for future investigation, including the onset of tube-chaotic transitions, Lyapunov analysis of the $\alpha_2(t)$ dynamics, and the classification of non-compact invariant geometries in higher-dimensional systems.

Acknowledgments

The author would like to thank Serge Bouquet (CEA, France) for many discussions on the special, torus-integrable case $\varepsilon = 0$, which laid the foundation for the present analysis. I am also grateful to Christoph Lhotka (University of Rome) for many years of continuous scientific exchange, and to Gilbert Guignard (CERN) for introducing me to nonlinear particle dynamics and for numerous insights into the geometric interpretation of invariants.

A special acknowledgment is due to my former mathematics teacher Heribert Hartmann, whose early guidance made it possible for me to pursue mathematics at all.

Finally, I would like to acknowledge the assistance provided by **OpenAI’s GPT-5 model**, whose contributions in structuring, clarifying and refining the presentation were of significant help during the preparation of this work.

References

- [1] J. Hagel, S. Bouquet, *Integrals for a special class of second order equations with a quadratic nonlinearity*, CERN SL/92-52 (AP), 1992.
- [2] H. R. Lewis, Classical and quantum systems with time-dependent harmonic-oscillator-type Hamiltonians, *Phys. Rev. Lett.* **18**, 510–512 (1967).
- [3] V. P. Ermakov, Second-order differential equations: Conditions of complete integrability, *Univ. Izv. Kiev* **9**, 1–25 (1880). (English translation: *Appl. Anal. Discrete Math.* **2**, 123–145 (2008).)
- [4] E. Pinney, The nonlinear differential equation $y'' + p(t)y + cy^{-3} = 0$, *Proc. Amer. Math. Soc.* **1**, 681 (1950).
- [5] G. W. Hill, On the part of the motion of the lunar perigee which is a function of the mean motions of the sun and moon, *Acta Math.* **8**, 1–36 (1886).
- [6] G. Floquet, Sur les équations différentielles linéaires à coefficients périodiques, *Ann. Sci. École Norm. Sup.* **12**, 47–88 (1883).
- [7] V. I. Arnold, *Mathematical Methods of Classical Mechanics*, Springer, 2nd edition (1989).
- [8] C. M. Bender and S. A. Orszag, *Advanced Mathematical Methods for Scientists and Engineers*, McGraw–Hill (1978).
- [9] F. W. J. Olver, *Asymptotics and Special Functions*, Academic Press (1974).
- [10] M. V. Berry, Uniform asymptotic smoothing of Stokes discontinuities, *Proc. Roy. Soc. Lond. A* **422**, 7–21 (1989).
- [11] J. A. Sanders, F. Verhulst, and J. Murdock, *Averaging Methods in Nonlinear Dynamical Systems*, Springer, 3rd edition (2007).
- [12] A. H. Nayfeh, *Perturbation Methods*, Wiley (2000).
- [13] A. Lindstedt, Über die Integration der Differentialgleichungen der Störungstheorie, *Math. Ann.* **9**, 424–434 (1876).